JOURNAL OF SPACECRAFT AND ROCKETS
Vol. 45, No. 5, September–October 2008

Slosh Analysis for Teardrop Tank

M. Utsumi*
IHI Corporation, Yokohama 235-8501, Japan

DOI: 10.2514/1.35156

Sloshing in a teardrop tank is analyzed by extending a newly developed, computationally efficient, semi-analytical method to the case in which the static liquid domain is nonaxisymmetric. To determine the characteristic functions analytically, a circumferential coordinate is defined around a line that penetrates the liquid surface at near the center of it, and spherical coordinates are introduced for each subdivided section of the circumferential coordinate. The origin of the spherical coordinates is at the apex of the conical surface that is tangent to the tank wall at the contact line of the static liquid surface with the tank wall. The following two cases are considered: 1) the case in which the sloshing is subjected to the gravitational force due to the propulsive acceleration, and 2) the case in which separation of the slosh eigenfrequency is caused by the Coriolis force. For the first case, it is shown that the mechanical models in the two orthogonal directions in which the breadth of the liquid surface is maximum and minimum may exhibit difference for low liquid-filling levels. In the second case, a two-directional mechanical model is developed by taking into account the interaction between the slosh motions in the two orthogonal directions.

Nomenclature

a	=	radius of spherical part of tank
F	=	disturbed liquid surface
$\ddot{f}_x$, $\ddot{f}_y(t)$	=	accelerations of tank in x and y directions
g	=	gravitational acceleration
H_0	=	z_1 coordinate of the center of spherical part of tank
H_1	=	z_1 coordinate of the origin of slosh force reference coordinates (x, y, z)
k_{1x}, k_{1y}	=	spring constants of mechanical models
L_0	=	x_1 coordinate of the center of spherical part of tank
L_1	=	x_1 coordinate of the origin of slosh force reference coordinates (x, y, z)
l_{0x}, l_{0y}	=	z coordinates of fixed masses
l_{1x}, l_{1y}	=	z coordinates of slosh masses
M	=	static liquid surface
m_{0x}, m_{0y}	=	fixed masses
m_{1x}, m_{1y}	=	slosh masses
$\mathbf{N}_F$	=	unit normal vector of F pointing into liquid domain
$\mathbf{N}_W$	=	unit normal vector of W pointing outward from liquid domain
p_{dy}	=	dynamic pressure
p_{imp}	=	impulsive pressure
p_{slo}	=	slosh pressure
p_{st}	=	static pressure
R, θ, φ	=	spherical coordinates
$R_F(\theta, \varphi, t)$	=	R coordinate of disturbed liquid surface F
$R_M(\theta)$	=	R coordinate of undisturbed liquid surface M
$R_W(\theta)$	=	R coordinate of tank wall W
u_R, u_θ, u_φ	=	R, θ, and φ components of liquid displacement relative to tank
v_R, v_θ, v_φ	=	R, θ, and φ components of liquid velocity relative to tank
v_{x1}, v_{y1}, v_{z1}	=	x_1, y_1, and z_1 components of liquid velocity relative to tank
W	=	tank wall
(x, y, z)	=	slosh force reference coordinates
(x_{sp}, y_{sp}, z_{sp})	=	spherical coordinates reference coordinates
(x_{tk}, y_{tk}, z_{tk})	=	tank reference coordinates (z_{tk} is tank axis)
(x_1, y_1, z_1)	=	rotating coordinates (z_1 is direction of g)
α	=	angle between $-z$ and z_1 directions
α_{cone}	=	half the apex angle of conical part of tank (Fig. 1a)
α_{sp}	=	angle between z_{sp} and z_{tk} directions
α_{tk}	=	angle between $-z_{tk}$ and z_1 directions
ε	=	1 or -1 when the origin of the spherical coordinates is $+z_{sp}$ side or $-z_{sp}$ side, respectively [Eq. (1)]
ζ	=	liquid surface displacement
ρ	=	liquid density
Ω	=	angular frequency of rotation
ω_x, ω_y	=	slosh eigenfrequencies for the case in which Coriolis force is not considered
$\omega_{1,slo}$, $\omega_{2,slo}$	=	slosh eigenfrequencies separated by Coriolis force

I. Introduction

LIQUID sloshing in a reduced-gravity environment has become one of the major research interests in space engineering because sloshing significantly affects the dynamics of a space vehicle [1]. There have been a considerable number of studies made on slosh dynamics for cylindrical [2–6] and arbitrary axisymmetric [7–10] tanks. Generally, sloshing problems for cylindrical tanks are solved by analytical methods, whereas sloshing in arbitrary axisymmetric tanks is analyzed by numerical methods. In previous papers [11,12], the author presented a computationally efficient semi-analytical method that can be applied to arbitrary axisymmetric tanks. This method uses spherical coordinates whose origin is at the apex of the cone that is tangent to the tank at the contact line of the static liquid surface, thereby analytically determining the characteristic function of the sloshing irrespective of the generatrix shape of the tank. These works [11,12] presented slosh analyses for the case in which the static liquid domain is axisymmetric and confirmed that the theoretical predictions for the eigenfrequency are in good agreement with previous theoretical [8] and experimental [10,13] results. The purpose of the present paper is to extend the semi-analytical method to a sloshing problem for a teardrop tank with a nonaxisymmetric shape of the static liquid domain. The geometry of a teardrop tank is shown in Fig. 1. By dint of the presence of the conical part and the tilt

Received 16 October 2007; revision received 19 February 2008; accepted for publication 24 February 2008.

*Senior Researcher, Machine Element Department, Technical Research Laboratory, 1 Shin-Nakaharacho, Isogo-ku, Kanagawa Prefecture; masahiko_utsumi@ihi.co.jp.

of the tank axis from the direction of the gravity, the liquid propellant can be held at the outlet (the apex of the conical part) for the case in which the tank undergoes the centrifugal and gravitational forces due to the rotation and the propulsion of the vehicle. In this paper, the following two cases are considered: 1) the case in which the sloshing is subjected to the gravitational force due to the propulsive acceleration, and 2) the case in which separation of the slosh eigenfrequency is caused by the Coriolis force. For the first case, we examine the difference between the mechanical models in the two orthogonal directions in which the breadth of the liquid surface is maximum and minimum is examined. In the second case, we encounter a problem that the conventionally used one-directional mechanical model for a certain direction of the tank excitation cannot be developed due to the interaction between the slosh motions in the two orthogonal directions. In this paper, a method for solving this problem is investigated. Such an investigation has not been conducted, although there exist many papers [14–18] for sloshing in a rotating tank. This paper develops a bidirectional model by taking into account the interaction between the slosh motions in the two orthogonal directions.

II. Method of Solution

A. Slosh Force Reference Coordinates

Figure 1 shows the mechanical models for the sloshing. The coordinates shown are fixed to the vehicle, and g is applied in the z_1 direction. The tank axis z_{tk} is tilted against the direction of g by the angle α_{tk} in the x_1z_1 plane to hold the liquid at the outlet (the apex of the conical part of the tank) for arbitrary relative magnitude of the gravitational and centrifugal forces. The slosh force reference coordinates (x, y, z) are defined, and the mass-spring mechanical models are developed to simulate the frequency responses of the x and y components of the slosh force and moment to the tank excitations $\ddot{f}_x(t)$ and $\ddot{f}_y(t)$ in the x and y directions. The slosh force reference coordinates (x, y, z) are defined by rotating the coordinates (x_1, y_1, z_1) by the angle $\pi + \alpha$ around the y_1 axis and shifting the origin to the position $(x_1, y_1, z_1) = (L_1, 0, H_1)$, where α, L_1, and H_1 are adjusted according to the relative magnitude of the gravitational and centrifugal forces, such that the x–y plane is nearly parallel to the static liquid surface, and the z axis penetrates the static liquid surface at near the center of it. The linear analysis is performed under the assumption that the liquid is incompressible and inviscid.

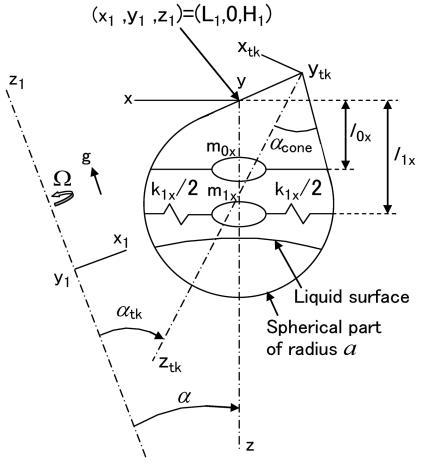

a) Mechanical model in x direction

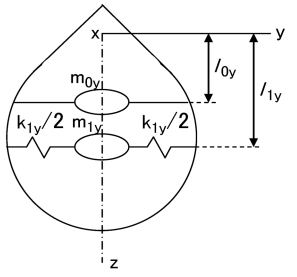

b) Mechanical model in y direction

Fig. 1 Mechanical models.

B. Spherical Coordinates

To extend the method developed in the previous works [11,12] to the sloshing problem with the nonaxisymmetric static liquid domain, we first define a circumferential coordinate φ around a line z_{sp} that is nearly a normal line of the static liquid surface at near the center of it. Second, for each divided section $\varphi_j \le \varphi \le \varphi_j + \Delta\varphi$ $(\Delta\varphi = 2\pi/N,\ \varphi_j = (j-1)\Delta\varphi,\ j = 1, 2, \ldots, N)$, we introduce spherical coordinates (R, θ, φ) such that

$$x_{sp} = R\sin\theta\cos\varphi, \qquad y_{sp} = R\sin\theta\sin\varphi, \qquad z_{sp} = h - \varepsilon R\cos\theta$$
$$(0 \le \theta \le \theta_{max}) \tag{1}$$

where the origin O $(z_{sp} = h)$ is the intersection of the z_{sp} axis and the line that is included in the plane $\varphi = \varphi_j$ and is tangent to the tank wall at the contact line of the static liquid surface with the tank wall. Figure 2 shows an example of the cross section of the liquid domain at the plane $\varphi = \varphi_j$ for the case in which $\varphi_j = \pi$. The spherical coordinates reference coordinates (x_{sp}, y_{sp}, z_{sp}) may be slightly changed from the slosh force reference coordinates (x, y, z) to improve the balance of the liquid mass around the z_{sp} axis. In terms of these spherical coordinates, the static liquid surface M, the disturbed liquid surface F, and the tank wall W in each section can be expressed as

$$M\colon\ R = R_M(\theta) \tag{2}$$

$$F\colon\ R = R_F(\theta, \varphi, t) = R_M(\theta) + \zeta(\theta, \varphi, t) \tag{3}$$

$$W\colon\ R = R_W(\theta) \tag{4}$$

The symbol j, representing the section number, is omitted to keep the notations uncomplicated. The functions $R_M(\theta)$ and $R_W(\theta)$ are derived by hand calculations. The oscillatory displacement ζ of the liquid surface is defined in the R direction. Therefore, the liquid surface displacement at the tank wall can be made tangential to the

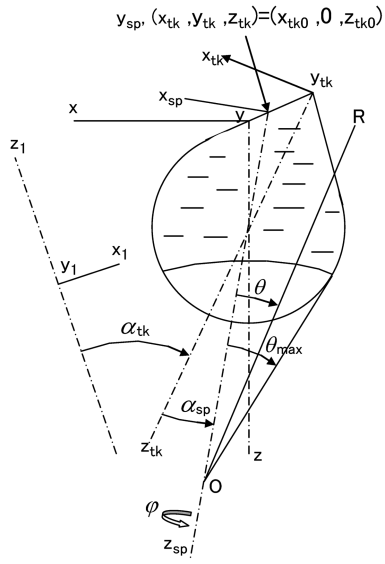

Fig. 2 Example of R and θ coordinates in a cross section $\varphi = \varphi_j$ of the liquid (the case in which $\varphi_j = \pi$).

tank wall, thereby satisfying the compatibility condition for the surface displacement.

In a previous paper [19], the tank reference coordinates (x_{tk}, y_{tk}, z_{tk}) were used as the spherical coordinates reference coordinates (x_{sp}, y_{sp}, z_{sp}) and the slosh force reference coordinates (x, y, z), and the mechanical models were developed for tank excitations in the x_{tk} and y_{tk} directions. However, a mechanical model is generally developed for a tank excitation parallel to a static liquid surface. Furthermore, the axis z_{sp} of the spherical coordinates should be nearly a normal line of the liquid surface at near the center of it and may be a little changed from the z axis to improve the balance of the liquid mass around the axis of the spherical coordinates. These considerations provide the impetus for this study.

C. Static Liquid Surface

Integrating the equilibrium conditions $(\partial p_{st}/\partial x_1, \partial p_{st}/\partial y_1, \partial p_{st}/\partial z_1) = (\rho\Omega^2 x_1, \rho\Omega^2 y_1, \rho g)$ between the pressure gradient and the body forces leads to

$$p_{st} = \rho[g z_1 + (1/2)\Omega^2(x_1^2 + y_1^2)] + C_1 \tag{5}$$

where C_1 is an arbitrary constant. From the condition that p_{st} vanishes over the liquid surface, the geometry of the static liquid surface M can be determined as

$$z_1 = -(\Omega^2/2g)(x_1^2 + y_1^2) - (C_1/\rho g) \tag{6}$$

The constant C_1 can be determined from the volume of the liquid. Equation (6) shows that the static liquid surface is a parabolic surface.

D. Mechanical Model Under Gravitational and Centrifugal Forces

When the Coriolis force is not included, the equations of motion of the liquid are given by

$$\partial v_{x_1}/\partial t + (1/\rho)\partial p_{dy}/\partial x_1 + \ddot{f}_x(t)\partial x/\partial x_1 + \ddot{f}_y(t)\partial y/\partial x_1 = 0 \tag{7a}$$

$$\partial v_{y_1}/\partial t + (1/\rho)\partial p_{dy}/\partial y_1 + \ddot{f}_x(t)\partial x/\partial y_1 + \ddot{f}_y(t)\partial y/\partial y_1 = 0 \tag{7b}$$

$$\partial v_{z_1}/\partial t + (1/\rho)\partial p_{dy}/\partial z_1 + \ddot{f}_x(t)\partial x/\partial z_1 + \ddot{f}_y(t)\partial y/\partial z_1 = 0 \tag{7c}$$

The last two terms of each equation represent the x_1, y_1, and z_1 components of the tank acceleration. The dynamic pressure p_{dy} can be decomposed into the slosh and impulsive pressures:

$$p_{dy} = p_{slo} + p_{imp} \tag{8}$$

The impulsive pressure p_{imp} results from the inertial force of the liquid due to the tank excitation and is given by

$$p_{imp} = -\rho[\ddot{f}_x(t)(x - x_0) + \ddot{f}_y(y - y_0)] \tag{9}$$

where x_0 and y_0 are determined such that the mean value of p_{imp} over the liquid surface vanishes. Using Eqs. (8) and (9), Eq. (7) can be transformed into

$$(\partial/\partial t)\{v_{x_1}, v_{y_1}, v_{z_1}\}^T = -\mathrm{grad}(p_{slo}/\rho) \tag{10}$$

which means that a velocity potential ϕ defined by $\partial\phi/\partial t = -p_{slo}/\rho$ exists. Therefore, the following variational principle [11] expressed in terms of ϕ can be used:

$$\int_{t_1}^{t_2}\left[\rho_f \iiint_V E_1\delta\phi\,\mathrm{d}V - \rho_f \iint_W E_2\delta\phi\,\mathrm{d}W - \rho_f \iint_F E_3\delta\phi\,\mathrm{d}F - \iint_F E_4\delta\zeta\cos(\mathbf{N}_F, R)\,\mathrm{d}F - \rho_f\delta G\cdot E_5\right]\mathrm{d}t = 0 \tag{11}$$

where

$$E_1 = \nabla^2\phi, \qquad E_2 = \nabla\phi\cdot\mathbf{N}_W,$$
$$E_3 = (\partial\zeta/\partial t)\cos(\mathbf{N}_F, R) - \nabla\phi\cdot\mathbf{N}_F, \qquad E_4 = p_{st} + p_{slo} + p_{imp},$$
$$E_5 = \iint_F (\partial\zeta/\partial t)\cos(\mathbf{N}_F, R)\,\mathrm{d}F \tag{12}$$

Because the variations $\delta\phi$, $\delta\zeta$, and δG are arbitrary and independent, Eq. (11) yields the governing equation $E_1 = 0$, the boundary conditions $E_i = 0$ $(i = 2\text{–}4)$, and the liquid volume constant condition $E_5 = 0$. The liquid volume constant condition can be derived from the other kinematic conditions using the Gauss theorem, and so it is not included in the subsequent analysis.

For the convenience of the slosh analysis in Sec. II.E, we introduce the fluid oscillatory displacement $\mathbf{u} = \{u_R, u_\theta, u_\varphi\}^T$, substitute $\nabla\phi = \partial\mathbf{u}/\partial t$ and

$$\delta\phi = \int(-\delta p_{slo}/\rho)\,\mathrm{d}t$$

into Eq. (11), and integrate by parts with respect to t. Expressing the normal vectors and the surface elements in terms of the spherical coordinates and using the linear approximation for the boundary conditions at the disturbed liquid surface, we finally obtain

$$\begin{aligned}&\int_0^{2\pi}\int_0^{\theta_{max}} \varepsilon\int_{R_M}^{R_W} \hat{E}_1\rho^{-1}\delta p_{slo}R^2\sin\theta\,\mathrm{d}R\,\mathrm{d}\theta\,\mathrm{d}\varphi\\ &+\int_0^{2\pi}\int_0^{\theta_{max}} (\hat{E}_2\rho^{-1}\delta p_{slo}|_{R=R_W}R_W\sin\theta\,\mathrm{d}\theta\,\mathrm{d}\varphi\\ &+\int_0^{2\pi}\int_0^{\theta_{max}} (\hat{E}_3\rho^{-1}\delta p_{slo}|_{R=R_M}\\ &+\hat{E}_4\delta\zeta\varepsilon R_M)R_M\sin\theta\,\mathrm{d}\theta\,\mathrm{d}\varphi = 0\end{aligned} \tag{13}$$

with

$$\hat{E}_1 = \mathrm{div}\mathbf{u} \tag{14a}$$

$$\hat{E}_2 = \varepsilon[-R_W u_R|_{R=R_W} + (\mathrm{d}R_W/\mathrm{d}\theta)u_\theta|_{R=R_W}] \tag{14b}$$

$$\hat{E}_3 = \varepsilon[R_M u_R|_{R=R_M} - (\mathrm{d}R_M/\mathrm{d}\theta)u_\theta|_{R=R_M} - R_M\zeta] \tag{14c}$$

$$\begin{aligned}\hat{E}_4 = &-\rho^{-1}p_{slo}|_{R=R_M} + \zeta[g f_1(\theta,\varphi) + \Omega^2 f_2(\theta,\varphi)]\\ &+ (x - x_0)\ddot{f}_x(t) + (y - y_0)\ddot{f}_y(t)\end{aligned} \tag{14d}$$

where $f_1(\theta, \varphi)$ and $f_2(\theta, \varphi)$ are functions arising from substituting $R = R_M + \zeta$ [Eq. (3)] into p_{st} given by Eq. (5). To transform Eq. (13) into modal equations, the modal functions for p_{slo} and $\mathbf{u}$ are analytically expressed in the following form by using the spherical coordinates introduced in Sec. II.B:

$$\begin{Bmatrix} p_{slo}\\ u_R\\ u_\theta\\ u_\varphi\end{Bmatrix} = \sum_{m\geq 0}\sum_{k\geq 1}\sum_{l=1,2}\sum_{q=1,2} A_{mklq}\begin{Bmatrix} \rho a\omega^2 X_{mkl}(R)\Theta_{mk}(\theta)\Phi_{mq}(\varphi)\\ aX'_{mkl}(R)\Theta_{mk}(\theta)\Phi_{mq}(\varphi)\\ aX_{mkl}(R)\Theta'_{mk}(\theta)\Phi_{mq}(\varphi)/R\\ aX_{mkl}(R)\Theta_{mk}(\theta)\Phi'_{mq}(\varphi)/R\sin\theta\end{Bmatrix} e^{i\omega t} \tag{15}$$

$$-\varepsilon\zeta = \sum_{m\geq 0}\sum_{k\geq 1}\sum_{q=1,2} C_{mkq}\Theta_{mk}(\theta)\Phi_{mq}(\varphi)e^{i\omega t} \tag{16}$$

where A_{mklq} and C_{mkq} are unknown constants. To include the slosh motions in the x and y directions, $\Phi_{m1} = \cos m\varphi$ and $\Phi_{m2} = \sin m\varphi$ are introduced. The method of deriving the characteristic functions X_{mkl} and Θ_{mk} are explained in [11,12]. The variables X_{mk1} and X_{mk2} represent the solutions for two characteristic exponents of the R-dependent functions. For the spherical coordinates introduced in Sec. II.B, $\theta_{\max}$ is smaller than $\pi/2$ (see Fig. 2). Therefore, the widely used associated Legendre polynomials can not be used as the characteristic function Θ_{mk}. The solution of Θ_{mk} can be expressed in terms of a Gaussian hypergeometric series. Because this series converges over the range $0 \leq \theta < \pi$, and $\theta_{\max}$ does not exceed $\pi/2$ in the present analysis, the convergence is rapid.

Substituting Eqs. (15) and (16) into the variational principle (13), neglecting the excitation terms, and considering variations for the constants A_{mklq} and C_{mkq} leads to a standard eigenvalue problem for these constants, from which the modal functions can be determined.

We develop the mechanical models for the fundamental modes in the x and y directions. Because these models can be developed similarly, explanation is given for the model in the x direction shown in Fig. 1a. We first express the solutions in terms of the associated modal functions by altering $e^{i\omega t}$ and $\omega^2 e^{i\omega t}$ in Eqs. (15) and (16) to the modal coordinates $q_x(t)$ and $-\ddot{q}_x(t)$, respectively. We then substitute these solutions into Eq. (13) and consider variations for the modal coordinate. We can thus obtain the modal equation of the form

$$\bar{M}_x\ddot{q}_x + \bar{K}_x q_x = \bar{\beta}_x\ddot{f}_x(t), \quad \text{that is,} \quad \ddot{q}_x + \omega_x^2 q_x = \beta_x\ddot{f}_x(t) \tag{17}$$

where $\omega_x^2 = \bar{K}_x/\bar{M}_x$ and $\beta_x = \bar{\beta}_x/\bar{M}_x$. By substituting the solution for the slosh pressure and Eq. (9) into

$$\begin{Bmatrix} F_x \\ M_y \end{Bmatrix} = \iint_W (p_{\text{slo}} + p_{\text{imp}}) \begin{Bmatrix} (\mathbf{N}_W \cdot \mathbf{e}_x) \\ [(\mathbf{N}_W \cdot \mathbf{e}_x)z - (\mathbf{N}_W \cdot \mathbf{e}_z)x] \end{Bmatrix} \mathrm{d}W \tag{18}$$

we can express the slosh force and moment in terms of the modal coordinate as

$$F_x = A_x\ddot{q}_x + B_x\ddot{f}_x(t), \qquad M_y = C_x\ddot{q}_x + D_x\ddot{f}_x(t) \tag{19}$$

where A_x, B_x, C_x, and D_x are constants arising from the integration. Substituting the solution to Eq. (17) for the sinusoidal excitation $\ddot{f}_x(t) = \sin\omega_f t$ into Eq. (19) gives

$$F_x = [A_x\beta_x\omega_f^2 + B_x(\omega_f^2 - \omega_x^2)]\sin\omega_f t/(\omega_f^2 - \omega_x^2) \tag{20}$$

$$M_y = [C_x\beta_x\omega_f^2 + D_x(\omega_f^2 - \omega_x^2)]\sin\omega_f t/(\omega_f^2 - \omega_x^2) \tag{21}$$

For the mechanical model, the equation of motion for the slosh mass m_{1x} and the dynamical force and moment exerted on the tank are given by

$$m_{1x}\ddot{u} + k_{1x}u - m_{1x}\Omega^2\cos^2\alpha\cdot u = -m_{1x}\ddot{f}_x(t) \tag{22}$$

$$F_{x,\text{mech}} = k_{1x}u - m_{0x}\ddot{f}_x(t) \tag{23}$$

$$M_{y,\text{mech}} = k_{1x}l_{1x}u + m_{1x}(l_{1x}\Omega^2\cos 2\alpha + \Omega^2 L_1\sin\alpha + g\cos\alpha)u - m_{0x}l_{0x}\ddot{f}_x(t) \tag{24}$$

where the terms for the gravitational and centrifugal forces can be derived using the procedure explained in Appendix A. By calculating the responses of $F_{x,\text{mech}}$ and $M_{y,\text{mech}}$ to the excitation $\ddot{f}_x(t) = \sin\omega_f t$ and using the condition that these responses are equal to F_x and M_y given by Eqs. (20) and (21) for arbitrary excitation frequency ω_f, the parameters of the mechanical model can be determined as

$$m_{0x} = -A_x\beta_x - B_x \tag{25a}$$

$$m_{1x} = A_x\beta_x/(1 + \omega_x^{-2}\Omega^2\cos^2\alpha) \tag{25b}$$

$$k_{1x} = m_{1x}(\omega_x^2 + \Omega^2\cos^2\alpha) \tag{25c}$$

$$l_{0x} = (C_x\beta_x + D_x)/(-m_{0x}) \tag{25d}$$

$$l_{1x} = [C_x\beta_x\omega_x^2 - m_{1x}(\Omega^2 L_1\sin\alpha + g\cos\alpha)]/(k_{1x} + m_{1x}\Omega^2\cos 2\alpha) \tag{25e}$$

E. Separated Slosh Eigenfrequencies

The slosh eigenfrequencies ω_x and ω_y determined in Sec. II.D are close to each other and may be referred to as one slosh eigenfrequency $\omega_{0,\text{slo}}$ under the gravitational and centrifugal forces. This eigenfrequency separates to two values $\omega_{1,\text{slo}}$ and $\omega_{2,\text{slo}}$ due to the Coriolis force. The purpose of this section is to predict these two values. The equations of motion of the liquid are obtained by adding $-2\Omega v_{y_1}$ and $2\Omega v_{x_1}$ to the left-hand sides of Eqs. (7a) and (7b) respectively. Expressing Eqs. (7a–7c) in terms of the spherical coordinates introduced by Eq. (1) and adding the terms for the residuals of Eqs. (7a–7c) to the variational principle (13) yields

$$\begin{aligned}&\int_0^{2\pi}\int_0^{\theta_{\max}} \varepsilon\int_{R_M}^{R_W} (-\hat{E}_a\delta u_R - \hat{E}_b\delta u_\theta - \hat{E}_c\delta u_\varphi \\ &\quad + \hat{E}_1\rho^{-1}\delta p_{\text{dy}})R^2\sin\theta\,\mathrm{d}R\,\mathrm{d}\theta\,\mathrm{d}\varphi \\ &\quad + \int_0^{2\pi}\int_0^{\theta_{\max}} (\hat{E}_2\rho^{-1}\delta p_{\text{dy}}|_{R=R_W}R_W + \hat{E}_3\rho^{-1}\delta p_{\text{dy}}|_{R=R_M}R_M \\ &\quad + \hat{E}_4\delta\zeta\varepsilon R_M^2)\sin\theta\,\mathrm{d}\theta\,\mathrm{d}\varphi = 0\end{aligned} \tag{26}$$

where

$$\begin{aligned}\hat{E}_a &= \partial v_R/\partial t + 2\Omega(G_1 v_\theta + G_2 v_\varphi) + (1/\rho)\partial p_{\text{dy}}/\partial R \\ &\quad + \ddot{f}_x(t)\partial x/\partial R + \ddot{f}_y(t)\partial y/\partial R\end{aligned} \tag{27a}$$

$$\begin{aligned}\hat{E}_b &= \partial v_\theta/\partial t + 2\Omega(G_3 v_\varphi - G_1 v_R) + [(1/\rho)\partial p_{\text{dy}}/\partial\theta \\ &\quad + \ddot{f}_x(t)\partial x/\partial\theta + \ddot{f}_y(t)\partial y/\partial\theta]/R\end{aligned} \tag{27b}$$

$$\begin{aligned}\hat{E}_c &= \partial v_\varphi/\partial t - 2\Omega(G_2 v_R + G_3 v_\theta) + [(1/\rho)\partial p_{\text{dy}}/\partial\varphi \\ &\quad + \ddot{f}_x(t)\partial x/\partial\varphi + \ddot{f}_y(t)\partial y/\partial\varphi]/R\sin\theta\end{aligned} \tag{27c}$$

with

$$\begin{aligned}G_1(\theta,\varphi) &= (1/R)[(\partial y/\partial R)(\partial x/\partial\theta) - (\partial x/\partial R)(\partial y/\partial\theta)] \\ G_2(\theta,\varphi) &= (1/R\sin\theta)[(\partial y/\partial R)(\partial x/\partial\varphi) - (\partial x/\partial R)(\partial y/\partial\varphi)] \\ G_3(\theta,\varphi) &= (1/R^2\sin\theta)[(\partial y/\partial\theta)(\partial x/\partial\varphi) - (\partial x/\partial\theta)(\partial y/\partial\varphi)]\end{aligned} \tag{28}$$

Substituting

$$\begin{Bmatrix} u_R \\ u_\theta \\ u_\varphi \\ p_{\mathrm{dy}} \end{Bmatrix} = \sum_{m\geq 0}\sum_{k\geq 1}\sum_{l\geq 1}\sum_{q=1,2} \begin{Bmatrix} \varepsilon a_{mklq}\Theta_{mk}(\theta) \\ b_{mklq}\Theta'_{mk}(\theta) \\ c_{mklq}\Theta_{mk}(\theta) \\ \rho a\omega^2 d_{mklq}\Theta_{mk}(\theta) \end{Bmatrix} \cos\left\{\frac{\pi(l-1)(R-R_M)}{(R_W-R_M)}\right\}\Phi_{mq}(\varphi)e^{i\omega t} \tag{29}$$

$$\zeta = -\varepsilon\sum_{m\geq 0}\sum_{k\geq 1}\sum_{q=1,2} e_{mkq}\Theta_{mk}(\theta)\Phi_{mq}(\varphi)e^{i\omega t} \tag{30}$$

into the variational principle (26) and considering variations with respect to the unknown constants a_{mklq}, b_{mklq}, c_{mklq}, d_{mklq}, and e_{mkq} leads to the matrix equation of the form

$$(-\omega^2\mathbf{M}_s + i\omega\mathbf{C}_s + \mathbf{K}_s)\mathbf{X}_s = \mathbf{F}_s \tag{31}$$

where $\mathbf{X}_s$ is the collection of the constants. The effect of the Coriolis force is represented by the term with the asymmetric matrix $\mathbf{C}_s$. By solving Eq. (31) and searching for resonance peaks, we can know the required slosh eigenfrequencies $\omega_{1,\mathrm{slo}}$ and $\omega_{2,\mathrm{slo}}$.

F. Model for Case with Separation of Eigenfrequency

We consider a mass m_1 connected to the tank with springs k_{1x} and k_{1y} in the x and y directions, respectively. The equations of motion of this mass can be derived as follows using the procedure explained in Appendix B:

$$\begin{aligned} &m_1\ddot{u} + 2m_1\Omega\dot{v}\cos\alpha + (k_{1x} - m_1\Omega^2\cos^2\alpha)u = -m_1\ddot{f}_x(t) \\ &m_1\ddot{v} - 2m_1\Omega\dot{u}\cos\alpha + (k_{1y} - m_1\Omega^2)v = -m_1\ddot{f}_y(t) \end{aligned} \tag{32}$$

where u and v are the dynamical displacements in the x and y directions, respectively. Based on Eq. (32), Eq. (22) and its correspondence for the excitation in the y direction are modified to the following coupled model:

$$\begin{aligned} &m_{1x}\ddot{u} + 2m_{1y}\Omega S\dot{v}\cos\alpha + (k'_{1x} - m_{1x}\Omega^2\cos^2\alpha)u = -m_{1x}\ddot{f}_x(t) \\ &m_{1y}\ddot{v} - 2m_{1x}\Omega S\dot{u}\cos\alpha + (k'_{1y} - m_{1y}\Omega^2)v = -m_{1y}\ddot{f}_y(t) \end{aligned} \tag{33}$$

where S is a parameter for controlling the separation of the eigenfrequency caused by the interaction between the slosh motions in the x and y directions, while k'_{1x} and k'_{1y} are modified spring constants. The roots of the frequency equation for Eq. (33) coincide with $\omega_{1,\mathrm{slo}}$ and $\omega_{2,\mathrm{slo}}$ when

$$\begin{aligned} &\frac{(k'_{1x} - m_{1x}\Omega^2\cos^2\alpha)}{m_{1x}} + \frac{(k'_{1y} - m_{1y}\Omega^2)}{m_{1y}} \\ &\quad + 4\Omega^2\cos^2\alpha\cdot S^2 = \omega^2_{1,\mathrm{slo}} + \omega^2_{2,\mathrm{slo}} \end{aligned} \tag{34}$$

$$\frac{(k'_{1x} - m_{1x}\Omega^2\cos^2\alpha)}{m_{1x}}\cdot\frac{(k'_{1y} - m_{1y}\Omega^2)}{m_{1y}} = \omega^2_{1,\mathrm{slo}}\omega^2_{2,\mathrm{slo}} \tag{35}$$

Equation (35) requires the geometric mean of the eigenfrequencies of the system in Eq. (33) in the absence of the Coriolis force be equal to the geometric mean of $\omega_{1,\mathrm{slo}}$ and $\omega_{2,\mathrm{slo}}$ determined from Eq. (31). If k'_{1x} and k'_{1y} are replaced by k_{1x} and k_{1y}, respectively, in Eq. (35), this equation does not hold exactly. For this reason, the modified spring constants k'_{1x} and k'_{1y} are introduced. These constants can not be determined uniquely from Eq. (35). However, because

$$(k_{1x} - m_{1x}\Omega^2\cos^2\alpha)/m_{1x} \cong (k_{1y} - m_{1y}\Omega^2)/m_{1y}$$

holds, k'_{1x} and k'_{1y} are determined such that

$$\frac{(k'_{1x} - m_{1x}\Omega^2\cos^2\alpha)}{m_{1x}} = \frac{(k'_{1y} - m_{1y}\Omega^2)}{m_{1y}} = \omega_{1,\mathrm{slo}}\omega_{2,\mathrm{slo}} \tag{36}$$

By eliminating k'_{1x} and k'_{1y} from Eqs. (34) and (36), S can be expressed as

$$S^2 = (\omega_{2,\mathrm{slo}} - \omega_{1,\mathrm{slo}})^2/(4\Omega^2\cos^2\alpha) \tag{37}$$

It can be seen from Eq. (37) that the parameter S is determined from the separation of the eigenfrequency.

In Eq. (35), the masses m_{1x} and m_{1y} were not modified so as to not disturb the conservation of mass that requires $m_{1x} + m_{0x}$ and $m_{1y} + m_{0y}$ be equal to the liquid mass. The numerical results obtained by this semi-analytical method satisfy this conservation of mass. Furthermore, numerically determined m_{1x} and m_{1y} are close to each other for arbitrary liquid-filling levels. Discussions for the conservation of mass are presented in Appendix C.

The method mentioned here is based on the following considerations. For the sloshing, the centrifugal force augments the stiffness term [see the third term on the right-hand side of Eq. (14d)]. However, for the mechanical models, the centrifugal force decreases the stiffness term, as can be seen from Eq. (32). This is because if the slosh mass approaches the rotational axis due to the dynamical displacement u, the centrifugal force decreases, thereby resulting in the reverse dynamical force against the restoring force $k_{1x}u$ of the spring. Also, for the dynamical displacement v, the same discussion can be made. Thus, the influences of the centrifugal force on the sloshing system and the mechanical model are completely different. This requires the centrifugal force be taken into account at the initial stage of the development of the mechanical model. However, the effects of the Coriolis force on the sloshing and the mechanical model are similar. Both the vibration systems undergo the separation of the eigenfrequency. Hence, the relatively simple method can be used to modify the mechanical models to take into account the effect of the Coriolis force.

III. Numerical Examples

Numerical calculation is conducted for the following case: $a = 0.25$ m, $\alpha_{\mathrm{cone}} = 40$ deg, $\alpha_{\mathrm{tk}} = 43$ deg, $L_0 = 0.5$ m, $H_0 = 0$ m, $\rho = 1009$ kg/m^3, and $g = 2$ m/s^2. Figure 3 shows the parameters of the mechanical models for the case in which the tank is not rotating. The slosh force reference coordinates (x, y, z) shown in Fig. 1a are defined by $L_1 = 0.5$ m, $H_1 = 0.284$ m, and $\alpha = 0$ deg, while the spherical coordinates reference coordinates shown in Fig. 2 are determined by $x_{\mathrm{tk0}} = 0.14$ m, $z_{\mathrm{tk0}} = 0.17$ m, and $\alpha_{\mathrm{sp}} = 38$ deg. It can be seen from Fig. 3a that for lower liquid-filling levels, ω_x is smaller than ω_y. This is because the liquid surface is longer in the x direction than in the y direction due to the presence of the conical part and the tilt of the tank axis z_{tk} from the direction of the gravity. However, the difference between the slosh masses in the x and y directions is small for all liquid-filling levels, as can be seen from Fig. 3b. By examining the values of the parameters of concern, it was found that this result is not because the presence of the conical part can be neglected, but is due to the following: The parameter A_x in Eq. (19) is larger than its correspondence A_y for the y direction. However, $\bar{M}_x$ in Eq. (17), corresponding to the kinetic energy, is larger than $\bar{M}_y$ so that $\beta_x = \bar{\beta}_x/\bar{M}_x$ becomes smaller than its correspondence β_y. Thus, from Eq. (25b), $m_{1x} \cong m_{1y}$ holds.

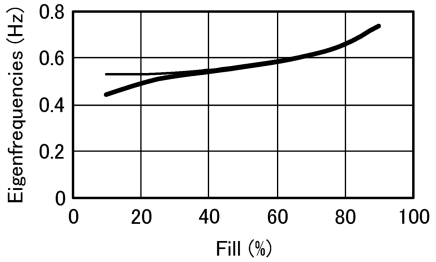

a) Eigenfrequencies (_____ , $\omega_x / 2\pi$; _____ , $\omega_y / 2\pi$)

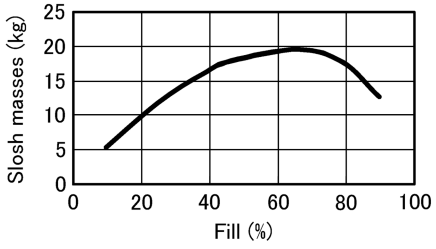

b) Slosh masses (_____ , m_{1x} ; _____ , m_{1y})

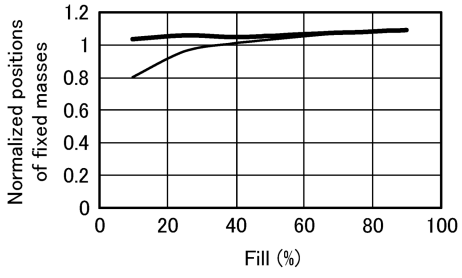

c) Normalized positions of fixed masses (_____ , l_{0x} / a ; _____ , l_{0y} / a)

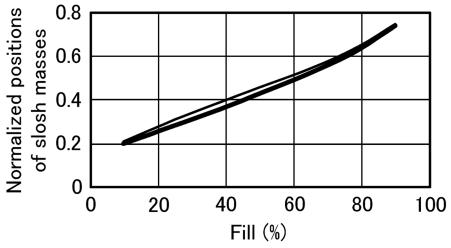

d) Normalized positions of slosh masses (_____ , l_{1x} / a ; _____ , l_{1y} / a)

Fig. 3 Parameters of mechanical models under gravitational force.

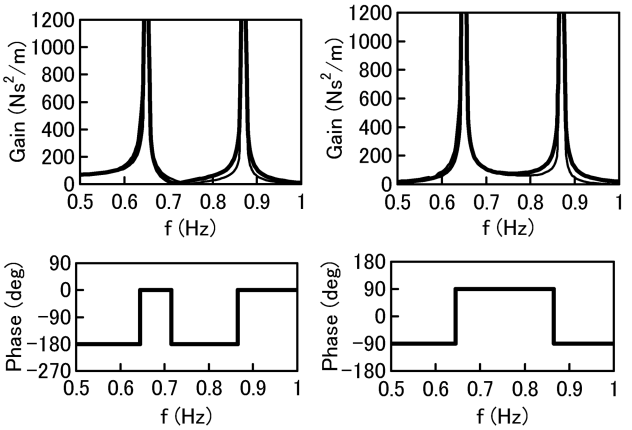

a) Force in x direction b) Force in y direction

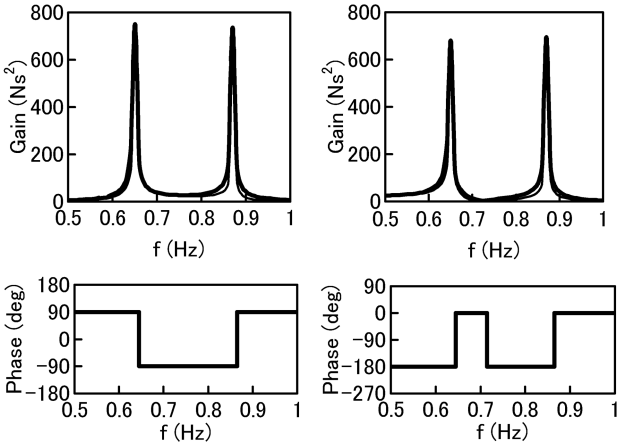

c) Moment in x direction d) Moment in y direction

Fig. 4 Responses to excitation $[\ddot{f}_x(t), \ddot{f}_y(t)] = (1, 0)e^{i2\pi ft}$ with separation of eigenfrequency due to rotation (liquid-filling level, 62%; thick line, mechanical model; thin line, sloshing system).

It can be seen from Fig. 3c that l_{0x} is larger than l_{0y} for low liquid-filling levels. The reason for this can be considered as follows: Because the integrand for C_x in Eq. (19) includes x, as can be seen from Eq. (18), and the liquid surface is longer in the x direction than in the y direction, C_x/C_y becomes larger than A_x/A_y in magnitude. Therefore, the first term $C_x\beta_x$ of the numerator on the right-hand side of Eq. (25d) becomes larger than $C_y\beta_y$. Furthermore, the fixed mass m_{0x} in the denominator of Eq. (25d) satisfies $m_{0x} \cong m_{0y}$ from the relation $m_{1x} \cong m_{1y}$ mentioned previously, and the conservation of mass that requires $m_{1x} + m_{0x}$ and $m_{1y} + m_{0y}$ be equal to the liquid mass. Thus, $l_{0x} > l_{0y}$ holds.

For l_{1x}, Eq. (25e) can be transformed into $l_{1x} = C_x\beta_x/m_{1x} - g/\omega_x^2$ when $\Omega = 0$ and $\alpha = 0$. Because of the relations $C_x\beta_x > C_y\beta_y$, $m_{1x} \cong m_{1y}$, and $\omega_x < \omega_y$ mentioned previously, the difference between l_{1x} and l_{1y} becomes small, even for low liquid-filling levels, as is shown in Fig. 3d.

Figures 4 and 5 show the frequency characteristics of the force and moment computed from the sloshing system in Eq. (31) and the mechanical model in Eq. (33) for the case in which the separation of the eigenfrequency is caused by rotation $\Omega = 20$ rpm. The tank reference coordinates (x_{tk}, y_{tk}, z_{tk}) are used as the slosh force reference coordinates and the spherical coordinates reference coordinates because the nonaxisymmetry of the static liquid domain around the tank axis is weak in contrast to the earlier case. It can be seen from Figs. 4 and 5 that the mechanical model can simulate the following characteristics of the sloshing system although complete agreement could not be achieved near the bottom of the resonant peak at the higher eigenfrequency: First, due to the interaction between the slosh motions in the x and y directions, the tank excitation $\ddot{f}_x(t)$ results in the force in the y direction and the moment in the x direction as well as the force in the x direction and the moment in the y direction. Second, the force in the y direction and the moment in the x direction caused by the interaction have no zero between the two separated eigenfrequencies, as can be seen from Figs. 4b and 4c. Furthermore, it is noted that the mechanical model can accurately simulate the complex change in the phase for x and y components of the force and moment over the frequency range covering the separated eigenfrequencies. For this reason, the thick and thin lines cannot be distinguished in the figures for the phase frequency characteristics.

The corresponding tendencies can be confirmed from Fig. 5 for the case of the tank excitation in the y direction. In this case, zero is not present between the two separated eigenfrequencies in the gain responses of the force in the x direction and the moment in the y direction that are caused by the interaction between the slosh motions in the x and y directions.

Figure 6 shows that the ratios k'_{1x}/k_{1x} and k'_{1y}/k_{1y} between the modified and original spring constants do not largely differ from unity over the wide range of the liquid-filling level. This means that the geometric mean of the eigenfrequencies of the system (33), in the absence of the Coriolis force, is near the geometric mean of the

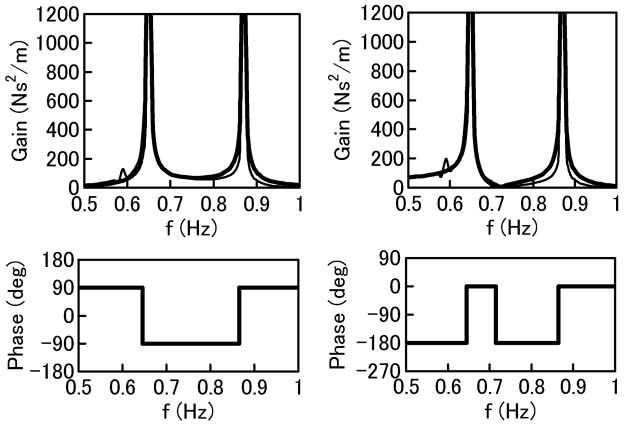

a) Force in x direction b) Force in y direction

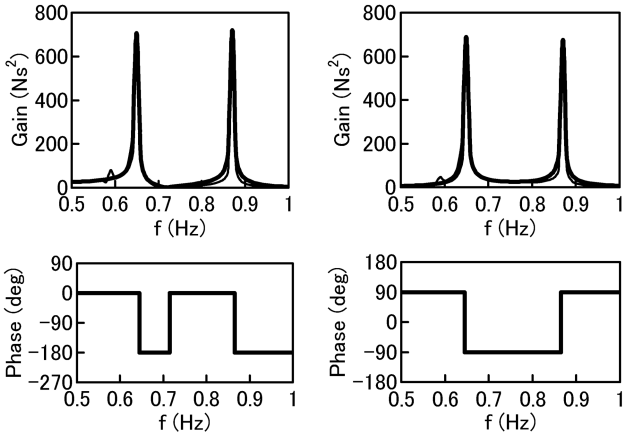

c) Moment in x direction d) Moment in y direction

Fig. 5 Responses to excitation $[\ddot{f}_x(t), \ddot{f}_y(t)] = (0, 1)e^{i2\pi ft}$ with separation of eigenfrequency due to rotation (liquid-filling level, 62%; thick line, mechanical model; thin line, sloshing system).

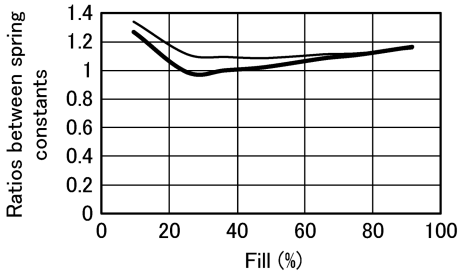

Fig. 6 The ratios between the modified and original spring constants (thick line, k'_{1x}/k_{1x}; thin line, k'_{1y}/k_{1y}).

eigenfrequencies $\omega_{1,\mathrm{slo}}$ and $\omega_{2,\mathrm{slo}}$ separated by the Coriolis force. However, as can be seen from Fig. 7, the parameter for controlling the separation of the eigenfrequency is smaller than unity and decreases with the increase in the liquid-filling level.

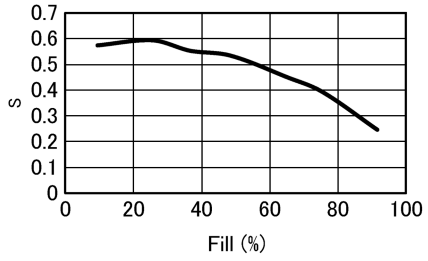

Fig. 7 Parameter S for controlling separation of eigenfrequency.

IV. Conclusions

A new semi-analytical method has been extended to a sloshing problem for a teardrop tank in which the static liquid domain is nonaxisymmetric. This extension can be made by defining a circumferential coordinate around a line that is nearly a normal line of the static liquid surface at near the center of it and introducing spherical coordinates for each subdivided section of the circumferential coordinate. The origin is at the apex of the conical surface that is tangent to the tank wall at the contact line of the static liquid surface with the tank wall. The following two cases were considered: 1) the case in which the sloshing is subjected to the gravitational force due to the propulsive acceleration, and 2) the case in which separation of the slosh eigenfrequency is caused by the Coriolis force. For the first case, it was illustrated that the mechanical models in the two orthogonal directions in which the breadth of the liquid surface is maximum and minimum become different for low liquid-filling levels. In the second case, we encounter a problem in that the conventionally used one-directional mechanical model for a certain direction of the tank excitation cannot be developed. One method for overcoming this difficulty was presented by developing the mechanical models in the two orthogonal directions under the gravitational and centrifugal forces and introducing interaction terms in such a way as to simulate the separation of the eigenfrequency of the sloshing.

Appendix A: Derivation of Equations (22) and (24)

The disturbed position $\mathbf{x} = \{u, 0, l_{1x}\}^T$ of the slosh mass in the (x, y, z) coordinates can be transformed into the (x_1, y_1, z_1) coordinates by

$$\begin{Bmatrix} x_1 \\ y_1 \\ z_1 \end{Bmatrix} = \begin{bmatrix} \cos(x_1, x) & 0 & \cos(x_1, z) \\ 0 & 1 & 0 \\ \cos(z_1, x) & 0 & \cos(z_1, z) \end{bmatrix} \begin{Bmatrix} u \\ 0 \\ l_{1x} \end{Bmatrix} + \begin{Bmatrix} L_1 \\ 0 \\ H_1 \end{Bmatrix}$$
$$= \begin{bmatrix} -\cos\alpha & 0 & -\sin\alpha \\ 0 & 1 & 0 \\ \sin\alpha & 0 & -\cos\alpha \end{bmatrix} \begin{Bmatrix} u \\ 0 \\ l_{1x} \end{Bmatrix} + \begin{Bmatrix} L_1 \\ 0 \\ H_1 \end{Bmatrix} \tag{A1}$$

In the (x, y, z) coordinates, the body force vector acting on the slosh mass can be expressed as follows:

$$\mathbf{F} = \begin{bmatrix} -\cos\alpha & 0 & \sin\alpha \\ 0 & 1 & 0 \\ -\sin\alpha & 0 & -\cos\alpha \end{bmatrix} \begin{Bmatrix} m_{1x}\Omega^2 x_1 \\ m_{1x}\Omega^2 y_1 \\ m_{1x} g \end{Bmatrix} \tag{A2}$$

The matrix in Eq. (A2) is the transposed matrix of the matrix in Eq. (A1). Substituting Eq. (A1) into Eq. (A2), we find that the dynamical x component of $-\mathbf{F}$ is equal to the third term on the left-hand side of Eq. (22), whereas the dynamical y component of the moment $\mathbf{x} \times \mathbf{F}$ coincides with the second term on the right-hand side of Eq. (24).

Appendix B: Derivation of Equation (32)

Because the space-fixed coordinates (X, Y, Z) are related to (x_1, y_1, z_1) by $X = x_1 \cos\Omega t - y_1 \sin\Omega t$, $Y = x_1 \sin\Omega t + y_1 \cos\Omega t$, and $Z = z_1$, the kinetic energy of the slosh mass can be expressed as

$$T = (1/2)m_1(\dot{X}^2 + \dot{Y}^2 + \dot{Z}^2) = (1/2)m_1[\dot{x}_1^2 + \dot{y}_1^2 + \dot{z}_1^2 + \Omega^2(x_1^2 + y_1^2) + 2\Omega(x_1\dot{y}_1 - \dot{x}_1 y_1)] \tag{B1}$$

Using Eq. (A1), we transform the position vector $\{u, v, l_1\}^T$ of the slosh mass in the (x, y, z) coordinates into the (x_1, y_1, z_1) coordinates. Substituting the resulting equation into Eq. (B1), using the Lagrange equations

$$(d/\mathrm{d}t)(\partial T/\partial \dot{u}) - \partial T/\partial u = -k_{1x}u - m_1 \ddot{f}_x(t),$$
$$(d/\mathrm{d}t)(\partial T/\partial \dot{v}) - \partial T/\partial v = -k_{1y}v - m_1 \ddot{f}_y(t) \tag{B2}$$

and neglecting the static terms, we obtain Eq. (32). The right-hand sides of Eq. (B2) represent the generalized forces.

Appendix C: Discussions for Conservation of Mass

From Eqs. (25a) and (25b), the sum of the slosh and fixed masses can be calculated as

$$m_{1x} + m_{0x} = -B_x - \frac{A_x \beta_x \Omega^2 \cos^2\alpha}{\omega_x^2 + \Omega^2 \cos^2\alpha} \tag{C1}$$

which is required be equal to the liquid mass. From Eqs. (9), (18), and (19), B_x is given by

$$-B_x = \iint_W \rho(x - x_0)\mathbf{N}_W \cdot \mathbf{e}_x \,\mathrm{d}W \tag{C2}$$

By using the Gauss theorem, Eq. (C2) can be transformed into

$$-B_x = \iiint_V \mathrm{div}[\rho(x - x_0)\mathbf{e}_x]\,\mathrm{d}V + \iint_M \rho(x - x_0)\mathbf{N}_M \cdot \mathbf{e}_x \,\mathrm{d}M \tag{C3}$$

The first term on the right-hand side of Eq. (C3) equals the liquid mass. When $\Omega = 0$, the liquid surface is a plane and $\mathbf{N}_M \cdot \mathbf{e}_x$ is constant over the liquid surface. Hence, the second term on the right-hand side of Eq. (C3) vanishes from the condition that the mean value of p_{imp} given by Eq. (9) over M is zero. Thus, the conservation of mass can be ascertained. When the tank rotation is present, the liquid surface concaves, and the second term on the right-hand side of Eq. (C3) is positive because $\mathbf{N}_M$ is pointing into the liquid domain. Therefore, $-B_x$ becomes larger than the liquid mass. However, $A_x\beta_x$ in Eq. (C1) is positive because the slosh force given by Eq. (20) is out of phase with the tank acceleration for an excitation frequency lower than the resonant frequency ω_x. Consequently, the value of the right-hand side of Eq. (C1) is very close to the liquid mass. In fact, this conservation of mass is satisfied by the values of the fixed and slosh masses numerically computed based on the present theory.

References

[1] Abramson, H. N. (ed.), "The Dynamic Behavior of Liquids in Moving Containers," NASA SP-106, Chap. 11, 1966.

[2] Dodge, F. T., and Garza, L. R., "Experimental and Theoretical Studies of Liquid Sloshing at Simulated Low Gravity," *Journal of Applied Mechanics*, Vol. 34, Sept. 1967, pp. 555–562.

[3] Bauer, H. F., and Eidel, W., "Linear Liquid Oscillations in Cylindrical Container Under Zero-Gravity," *Applied Microgravity Technology*, Vol. 2, No. 4, 1990, pp. 212–220.

[4] Bauer, H. F., and Eidel, W., "Hydroelastic Vibrations in a Circular Cylindrical Container with a Flexible Bottom in Zero-Gravity," *Journal of Fluids and Structures*, Vol. 7, No. 7, 1993, pp. 783–802. doi:10.1006/jfls.1993.1046

[5] Yuanjun, H., Xingrui, M., Pingping, W., and Benli, W., "Low-Gravity Liquid Nonlinear Sloshing Analysis in a Tank Under Pitching Excitation," *Journal of Sound and Vibration*, Vol. 299, No. 1, 2007, pp. 164–177. doi:10.1016/j.jsv.2006.07.003

[6] Peterson, L. D., Crawley, E. F., and Hansman, R. J., "Nonlinear Fluid Slosh Coupled to the Dynamics of a Spacecraft," *AIAA Journal*, Vol. 27, No. 9, 1989, pp. 1230–1240.

[7] Chu, W. H., "Low-Gravity Fuel Sloshing in an Arbitrary Axisymmetric Rigid Tank," *Journal of Applied Mechanics*, Vol. 37, Sept. 1970, pp. 828–837.

[8] Concus, P., Crane, G. E., and Satterlee, H. M., "Small Amplitude Lateral Sloshing in Spheroidal Containers Under Low Gravitational Conditions," NASA CR-72500, 1969.

[9] Dodge, F. T., Green, S. T., and Cruse, M. W., "Analysis of Small-Amplitude Low Gravity Sloshing in Axisymmetric Tanks," *Microgravity Science and Technology*, Vol. 4, No. 4, 1991, pp. 228–234.

[10] Dodge, F. T., and Garza, L. R., "Simulated Low-Gravity Sloshing in Spherical, Ellipsoidal, and Cylindrical Tanks," *Journal of Spacecraft and Rockets*, Vol. 7, No. 2, 1970, pp. 204–206.

[11] Utsumi, M., "Low-Gravity Propellant Slosh Analysis Using Spherical Coordinates," *Journal of Fluids and Structures*, Vol. 12, No. 1, 1998, pp. 57–83. doi:10.1006/jfls.1997.0125

[12] Utsumi, M., "Low-Gravity Sloshing in an Axisymmetrical Container Excited in the Axial Direction," *Journal of Applied Mechanics*, Vol. 67, June 2000, pp. 344–354. doi:10.1115/1.1307500

[13] Coney, T. A., and Salzman, J. A., "Lateral Sloshing in Oblate Spheroidal Tanks Under Reduced and Normal Gravity Conditions," NASA TN D-6250, 1971.

[14] Miles, J. W., and Troesch, B. A., "Surface Oscillations of a Rotating Liquid," *Journal of Applied Mechanics*, Vol. 28, Dec. 1961, pp. 491–496.

[15] Weihs, D., and Dodge, F. T., "Liquid Motions in Nonaxisymmetric, Partially Filled Containers Rotating at Zero Gravity," *Journal of Spacecraft and Rockets*, Vol. 28, No. 4, 1991, pp. 425–432.

[16] Bauer, H. F., "Response of a Rotating Finite Annular Liquid Layer to Various Axial Excitations in Zero Gravity," *Journal of Sound and Vibration*, Vol. 149, No. 2, 1991, pp. 219–234. doi:10.1016/0022-460X(91)90632-T

[17] Bauer, H. F., "Hydroelastic Oscillations of Rotating Liquid-Structure Systems in Zero Gravity," *Journal of Fluids and Structures*, Vol. 6, No. 5, 1992, pp. 603–632. doi:10.1016/0889-9746(92)90021-T

[18] El-Raheb, M., and Wagner, P., "Vibration of a Liquid With a Free Surface in a Spinning Spherical Tank," *Journal of Sound and Vibration*, Vol. 76, No. 1, 1981, pp. 83–93. doi:10.1016/0022-460X(81)90293-5

[19] Utsumi, M., "Development of Mechanical Models for Propellant Sloshing in Teardrop Tanks," *Journal of Spacecraft and Rockets*, Vol. 37, No. 5, 2000, pp. 597–603.

L. Peterson
Associate Editor